

Electrical characteristics of p^+ -Ge/(N -GaAs and N -AlGaAs) junctions and their applications to Ge base transistors

M. S. Ünlü, S. Strite, G. B. Gao, K. Adomi, and H. Morkoç
Materials Research Laboratory & Coordinated Science Laboratory, 1101 West Springfield Avenue,
University of Illinois at Urbana-Champaign, Urbana, Illinois 61801

(Received 8 September 1989; accepted for publication 20 December 1989)

Electrical properties of p^+ -Ge/ N -AlGaAs (and N -GaAs) are studied as a function of temperature and current conduction mechanisms are outlined. Junctions with Ge grown on GaAs and AlGaAs show ideality factors of unity and 1.03 at room temperature, respectively. Temperature-dependent current-voltage (I - V) and room-temperature capacitance-voltage (C - V) characterization are employed to determine the built-in voltage (V_{bi}) of the two diode structures. For Ge/GaAs, a valence-band discontinuity of 0.49 ± 0.05 eV is measured which is in good agreement with the value deduced from photoemission studies. Implications of p^+ -Ge base in AlGaAs/Ge/GaAs double-heterojunction bipolar transistors (DHBTs) are discussed.

Since the inception of heterojunction bipolar transistors (HBTs), efforts have been under way to improve performance by means of different material systems and device structures. Critical parameters affecting device performance are base doping, base contact resistance, and band discontinuity at the base-emitter junction. The semiconductor germanium has excellent potential to improve the performance of GaAs/AlGaAs based HBTs. Ge has a higher hole mobility and can be doped more heavily than any other device grade semiconductor. Heavily doped Ge could be used as a low-resistance base for n - p - n HBTs in the GaAs material system.¹⁻³ Higher injection efficiencies and lower base contact resistances should be attainable since Ge has a smaller band gap than GaAs. An AlGaAs/Ge emitter-base structure would combine the large valence-band discontinuity with the large minority carrier diffusion length required for high performance n - p - n HBTs. Defect-free Ge can be grown epitaxially on GaAs (100)⁴⁻⁷ due to the nearly perfect lattice match between the two systems.

Earlier, we reported encouraging ideality factors for heavily doped Ge ($p = 1 \times 10^{19}$ cm⁻³) grown on lightly doped GaAs ($n = 7 \times 10^{16}$ cm⁻³).⁸ In this letter we extend this study to improved Ge/GaAs as well as p^+ -Ge/ N -AlGaAs heterojunctions. Excellent forward and reverse characteristics in present diode structures allowed the investigation of current transport mechanisms via the temperature dependence of current-voltage relationship. Capacitance-voltage and temperature-dependent I - V characteristics were used to determine the built-in voltages and the heterojunction band discontinuities. Nearly ideal characteristics of Ge/(Al)GaAs junctions suggest that this system can be incorporated in high performance HBTs. Preliminary results for an emitter up Al_{0.22}Ga_{0.78}As/Ge/GaAs N - p - n double heterojunction bipolar transistor (DHBT) obtained in our laboratory are encouraging with a dc current gain of over 250.

The (Al)GaAs growth was performed on a Perkin-Elmer 430 molecular beam epitaxy system while Ge growth took place in an adjacent deposition chamber. Samples remained under vacuum during the several minutes of growth interruption required for transfer between chambers. An initial buffer layer of 1 μ m Si-doped GaAs with a carrier concentration of $n = 5 \times 10^{18}$ cm⁻³ was grown on semi-insulat-

ing GaAs(100) substrates misoriented 4° towards [011]. For the AlGaAs/Ge heterojunction, 0.2 μ m of Al_{0.2}Ga_{0.8}As ($n = 5 \times 10^{17}$ cm⁻³) was deposited and then capped by a few monolayers of undoped GaAs, while the GaAs/Ge junction had 0.2 μ m of GaAs doped less heavily ($n = 5 \times 10^{16}$ cm⁻³). Nominally 500 Å of Ge was then deposited, the growth being interrupted several times for Ga delta doping. Total Ge doping concentration was determined by transmission line measurements to be $p \approx 10^{19}$ cm⁻³ and $p \approx 10^{18}$ cm⁻³ for Ge/AlGaAs and Ge/GaAs diodes, respectively.

After growth, diodes with various mesa sizes were fabricated by standard photolithographic and wet etching techniques. The n -type contacts were formed by evaporating AuGe/Ni/Au on n^+ -GaAs and alloying at 450 °C. Relying on its small band gap, p -type ohmic contacts for Ge formed by palladium plating.⁸

The diode structures discussed here have Ge grown on the III-V material in order to study the intrinsic properties of these junctions while avoiding the difficulties related to polar on nonpolar epitaxy. The Ge/GaAs diodes exhibit nearly ideal forward characteristics and low leakage reverse bias characteristics (leakage current density $\leq 8 \times 10^{-5}$ A/cm² at 5 V, and $\approx 5 \times 10^{-3}$ A/cm² at 15 V reverse bias) with a sharp breakdown at ≈ 17 V. The corresponding electric field at this breakdown voltage is 4.3×10^5 V/cm which approaches the theoretical breakdown for GaAs (4 - 5×10^5 V/cm).⁹ Hard breakdown characteristics in a p - n junction, as opposed to a soft breakdown characteristic,⁸ is one desirable property for good transistors, particularly for power devices.

Typical I - V characteristics of the p -Ge/ N -AlGaAs junction at various temperatures are shown in Fig. 1. At room temperature, the ideality factor is as low as 1.03 and minimum ideality factor range extends over 4-5 decades of current. This behavior suggests that current transport is due almost entirely to diffusion or thermionic emission. However, the ideality factor increases with decreasing temperature. In Fig. 2, the minimum ideality factor n and logarithmic slope constant $\alpha (= nkT/q)$ versus temperature for Ge/GaAs and Ge/AlGaAs junctions is plotted. The larger ideality factor for AlGaAs suggests that recombination and tunneling current components are more important than for Ge/GaAs. This is expected because of the higher doping

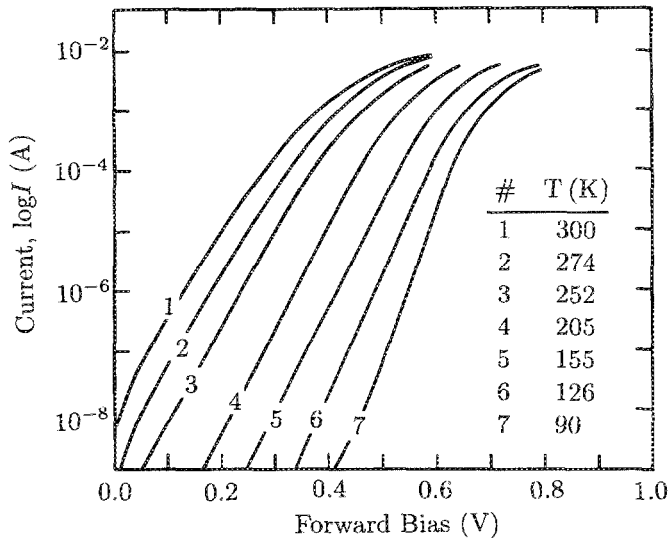


FIG. 1. Typical current-voltage characteristics of Ge/AlGaAs diodes at various temperatures (device size is $125 \times 75 \mu\text{m}^2$).

level and larger band discontinuity of the Ge/AlGaAs compared to Ge/GaAs. At low temperatures the AlGaAs heterojunction shows a dominant tunneling current as inferred from the ideality factor in excess of two and the almost constant α . The tunneling may be aided by imperfections across the conduction-band barrier.

Figure 3 shows the dependence of saturation current on inverse temperature for both diodes. Saturation current values are determined by extrapolating the minimum ideality factor range of I - V curves to intersect with the current axis. For an abrupt heterojunction, the dependence of the saturation current on the temperature T is given as $I_0 \propto \exp(-qV_{bi}/kT)$, i.e., $\log I_0 \propto V_{bi}/T$. Therefore, the slopes of the curves in Fig. 3 can be used to determine the corresponding V_{bi} values for the abrupt Ge/GaAs and Ge/AlGaAs junctions. The excellent linearity of data points in Fig. 3 is another indication of nearly pure thermionic current and high quality junctions. To further investigate the band alignment of these junctions, capacitance-voltage (C - V) measurements were also carried out. Built-in voltages were determined by means of the intercept method,¹⁰ i.e.,

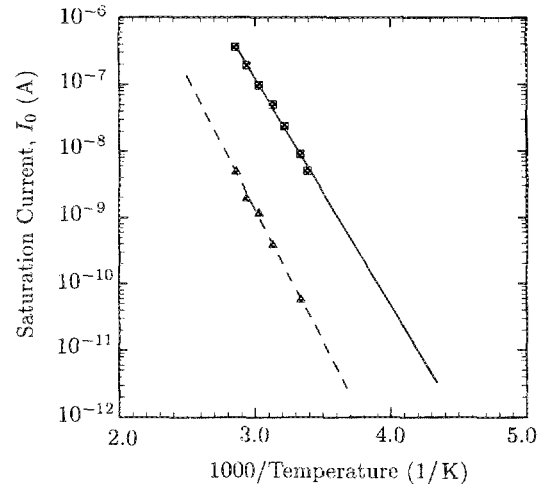


FIG. 3. Plots of logarithm of saturation current vs inverse of temperature for Ge/GaAs (\blacktriangle) and Ge/AlGaAs (\blacksquare) diodes (device sizes are $125 \times 75 \mu\text{m}^2$).

extrapolating linear $1/C^2$ versus reverse bias curves into the forward bias region and determining the intercept with the voltage axis V_{int} ($V_{bi} = V_{int} - 2kT/q$).

Table I lists the V_{bi} values determined by I - V and C - V measurements. The built-in voltage values from our C - V measurements were used to calculate the corresponding conduction- and valence-band discontinuities for the Ge/GaAs and Ge/AlGaAs diodes as

$$\Delta E_n = E_{gN} + kTF_{1/2}^{-1} \left(\frac{N_D}{N_{C_N}} \right) + kTF_{1/2}^{-1} \left(\frac{N_A}{N_{V_p}} \right) - qV_{bi}, \quad (1)$$

where $F_{1/2}^{-1}$ represents the inverse Fermi function; N_D and N_A are donor and acceptor densities, respectively; N_{C_N} and N_{V_p} are conduction- and valence-band density of states for N and p regions, respectively; and E_{gN} is the band gap of the N region. A comparison to Ge/GaAs valence-band discontinuity values obtained independently from synchrotron radiation photoemission¹¹ and x-ray photoemission spectroscopy^{12,13} is also included in Table I. We note good agreement of our results to within the experimental uncertainty with the published data. To the best of our knowledge, the only reported band discontinuity values for the AlGaAs/Ge system are from C - V measurements¹⁴ for a junction with an aluminum mole fraction of 0.17. This mole fraction is fairly close to our value of 0.2, and a direct comparison results in very good agreement (Table I).

The built-in voltage values deduced by I - V vs $1/T$ and C - V measurements will yield consistent results for abrupt junctions. In graded junctions over a distance much smaller than the depletion region, the built-in voltage as determined from C - V measurements should still be the same as in the abrupt case.¹⁵ For a graded junction, however, the I - V measurements will reflect the effective barrier height opposing the minority-carrier injection instead of the true built-in voltage. The current for N - p junctions is mainly due to electrons injected from large band-gap material; therefore, the effective barrier height will be determined by the conduction-band configuration.

As seen in Table I, very good agreement between I - V

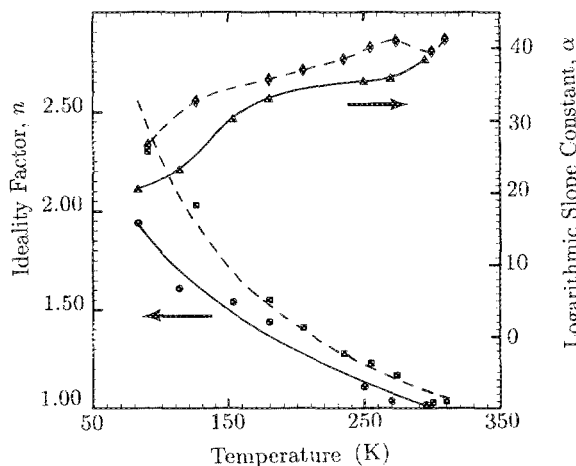


FIG. 2. Ideality factor and logarithmic slope constant for Ge/GaAs (solid) and Ge/AlGaAs (dashed) as a function of temperature. The curves are drawn to show the trend and do not represent any theoretical fit.

TABLE I. Band discontinuity and built-in voltage values determined from I - V and C - V measurements for Ge/GaAs and Ge/AlGaAs diodes in comparison with ΔE_v values from Refs. 11 and 12 for Ge/GaAs and band discontinuities from Ref. 14 for Ge/AlGaAs.

Diode		I - V	C - V	Ref. 11	Ref. 12	Ref. 14
Ge/GaAs	V_{bi} (V)	0.79	0.85 ± 0.03			
	ΔE_v (eV)		0.49 ± 0.05	0.46 ± 0.05	0.56 ± 0.04	
	ΔE_c (eV)		0.28 ± 0.05			
Ge/AlGaAs	V_{bi} (V)	0.66	1.00 ± 0.03			
	ΔE_v (eV)		0.69 ± 0.05			0.71
	ΔE_c (eV)		0.33 ± 0.05			0.31

and C - V methods exists for the Ge/GaAs case. This suggests a fairly abrupt junction relative to the GaAs depletion width of ≈ 1500 Å. As expected, the V_{bi} from C - V for Ge/AlGaAs is larger than that of Ge/GaAs. However, when deduced from I - V measurements with abrupt junction assumption, V_{bi} is considerably smaller for Ge/AlGaAs. This is most likely due to cross diffusion and resultant grading at the interface. Since the AlGaAs is more heavily doped than the GaAs in the Ge/GaAs diode, the depletion width is only ≈ 500 Å which corresponds to a conduction-band spike width above the Ge conduction band of ≈ 80 Å. If Ge diffusion into the AlGaAs were to exceed this 80 Å, the potential spike in the conduction band would be altered drastically. Such diffusion results in a reduced effective barrier ($\Delta\phi_{eff}$) opposing electron injection from AlGaAs into Ge since $\Delta\phi_{eff} = qV_{bi} - \Delta E_c$, ΔE_c being the conduction-band discontinuity. In this case, the saturation current dependence on temperature is $\log I_0 \propto \Delta\phi_{eff}/T$. The band discontinuity value obtained from C - V measurements is then used to determine $\Delta\phi_{eff} = 0.67$ eV, which is in agreement with that deduced from I - V measurements. The above argument can also be used to explain the slightly smaller V_{bi} values obtained from I - V measurements as compared to C - V in the Ge/GaAs case. However, since the depletion region is much wider, we expect only a small deviation from the actual barrier. For example, if we assume 100 Å of diffusion at the interface, the reduction of the conduction-band spike is less than 100 meV. This reduces the effective barrier to 0.75 ± 0.05 eV as compared to 0.79 eV determined from I - V measurements for the Ge/GaAs diode. Despite the agreement found through the nonabrupt interface discussion, other possibilities such as tunneling current for a heavily doped Ge/AlGaAs junction may play a part in deviations in the V_{bi} determined by I - V measurements. Tunneling will effectively reduce the barrier to minority carriers. Since the I - V measurements give the effective barrier height opposing the minority-carrier transport, measured values will be smaller than the true built-in voltage. Smaller V_{bi} deduced from I - V measurements for the Ge/AlGaAs diode compared to the Ge/GaAs can also be explained as the tunneling being more dominant for heavily doped junctions.

The measured valence-band discontinuity value for Ge/AlGaAs (0.69 eV) is much larger than that of GaAs/AlGaAs (0.10 eV)¹⁶ for the same Al mole fraction ($x = 0.2$). Therefore, a higher emitter injection efficiency γ [$\gamma \propto \exp(\Delta E_v/kT)$] can be expected from the AlGaAs/Ge emitter-base junction. Once the problems related to polar on nonpolar epitaxy are solved, this junction is a perfect candi-

date for high current gain HBTs.

In conclusion, we have demonstrated high quality p^+ -Ge/ N -(Al)GaAs diode structures grown by molecular beam epitaxy. Diode characteristics were studied by variable temperature I - V and room-temperature C - V measurements. Both diodes exhibited nearly ideal room-temperature current transport, while the AlGaAs diode showed a large recombination/defect-assisted tunneling current at low temperatures. From our measurements we deduced band discontinuity values which are in good agreement with the available data for Ge/GaAs and Ge/AlGaAs. The nearly ideal reverse breakdown characteristics for Ge/GaAs and forward current characteristics of Ge/AlGaAs junctions suggest Ge as an alternative to GaAs in AlGaAs/GaAs DHBTs to improve the present device performances.

This research is supported by the Air Force Office of Scientific Research (grant No. AFOSR-89-0239), by the SDIO IST office through ONR (grant No. N00014-86-K-0513), and the National Science Foundation (grant No. ECS-88-22406). Special thanks go to C. W. Litton, K. Evans, and Perkin Elmer for the loan of equipment instrumental to this investigation. One of us (S. S.) wishes to acknowledge the support of a NSF Graduate Fellowship. We would also like to thank the reviewer for constructive criticism.

¹D. K. Jadas and D. L. Feucht, IEEE Trans. Electron Devices ED-16, 102 (1969).

²N. Chand, J. Klem, and H. Morkoç, Appl. Phys. Lett. 48, 484 (1986).

³T. Kimura, M. Kawanaka, and J. Sone, Paper IIA-8, 47th Device Research Conference, June 19-21, Cambridge, MA, IEEE, 1989.

⁴R. S. Bauer and J. C. Mikkelsen, J. Vac. Sci. Technol. 21, 491 (1982).

⁵Chin-An Chang, J. Appl. Phys. 53, 1253 (1982).

⁶J. H. Neave, P. K. Larsen, B. A. Joyce, J. P. Gowers, and J. F. van der Veen, J. Vac. Sci. Technol. B 1, 668 (1983).

⁷S. Strite, D. Biswas, N. S. Kumar, M. Fradkin, and H. Morkoç, Appl. Phys. Lett. 56, 244 (1990).

⁸M. S. Ünlü, S. Strite, T. Won, K. Adomi, J. Chen, S. Noor Mohammad, D. Biswas, and H. Morkoç, Electron. Lett. 25, 1359 (1989).

⁹S. M. Sze, Semiconductor Devices Physics and Technology (Wiley, New York, 1976), p. 103.

¹⁰H. K. Gummel and D. L. Scharfetter, J. Appl. Phys. 38, 655 (1967).

¹¹P. Chiaradia, A. D. Katnani, H. W. Sang, Jr., and R. S. Bauer, Phys. Rev. Lett. 52, 1246 (1984).

¹²R. W. Grand, E. A. Kraut, J. R. Waldrop, and S. P. Kowalczyk, "Interface Contributions to Heterojunction Band Discontinuities: X-ray Photoemission Spectroscopy Investigations," in Heterojunction Band Discontinuities, Physics and Device Applications, edited by Federico Capasso and Giorgio Margaritondo (North-Holland, Amsterdam, 1987), p. 167.

¹³J. R. Waldrop and R. W. Grant, Phys. Rev. Lett. 43, 1686 (1979).

¹⁴D. S. Howarth and D. L. Feucht, Appl. Phys. Lett. 23, 365 (1973).

¹⁵R. Fischer, T. Henderson, J. Klem, and H. Morkoç, Solid-State Electron. 29, 193 (1986).

¹⁶R. C. Miller, A. C. Gossard, and D. A. Kleinman, Phys. Rev. B 32, 5443 (1985).